HHS Public Access

Author manuscript

Science. Author manuscript; available in PMC 2016 August 22.

Published in final edited form as:

Science. 2016 July 15; 353(6296): 300–305. doi:10.1126/science.aad4225.

Chromatin Remodeling Inactivates Activity Genes and Regulates Neural Coding

Yue Yang[#1], **Tomoko Yamada**[#1,‡], **Kelly K. Hill**[1,2], **Martin Hemberg**[3], **Naveen C. Reddy**[1], **Ha Y. Cho**[1], **Arden N. Guthrie**[1], **Anna Oldenborg**[1], **Shane A. Heiney**[4], **Shogo Ohmae**[4], **Javier F. Medina**[4], **Timothy E. Holy**[1], and **Azad Bonni**[1,*]

[1]Department of Neuroscience, Washington University School of Medicine, St. Louis, MO 63110, USA

[2]MD-PhD Program, Washington University School of Medicine, St. Louis, Missouri, 63110, USA

[3]Wellcome Trust Sanger Institute, Hinxton CB10 1SA, UK

[4]Department of Neuroscience, Baylor College of Medicine, Houston, TX 77030, USA

[#] These authors contributed equally to this work.

Abstract

Activity-dependent transcription influences neuronal connectivity, but the roles and mechanisms of inactivation of activity-dependent genes have remained poorly understood. Genome-wide analyses in the mouse cerebellum revealed that the nucleosome remodeling and deacetylase (NuRD) complex deposits the histone variant H2A.z at promoters of activity-dependent genes, thereby triggering their inactivation. Purification of translating mRNAs from synchronously developing granule neurons (Sync-TRAP) showed that conditional knockout of the core NuRD subunit Chd4 impairs inactivation of activity-dependent genes when neurons undergo dendrite pruning. Chd4 knockout or expression of NuRD-regulated activity genes impairs dendrite pruning. Imaging of behaving mice revealed hyperresponsivity of granule neurons to sensorimotor stimuli upon Chd4 knockout. Our findings define an epigenetic mechanism that inactivates activity-dependent transcription and regulates dendrite patterning and sensorimotor encoding in the brain.

Neuronal activity influences transcription in neurons, and hence regulates neural circuits (1-2). Activity-dependent genes are often rapidly transcribed and then rapidly inactivated (3-4). However, attention has focused on the induction of transcription (1, 5-7) rather than the biological roles and mechanisms of inactivation of activity-dependent transcription.

[*]To whom correspondence should be addressed. bonni@wustl.edu.

[‡]Present address: Faculty of Medicine, University of Tsukuba, Tsukuba, Ibaraki, 305-8575, Japan

The authors declare no conflicts of interest.

Supplementary Materials
Materials and Methods
Figs. S1 to S10
Tables S1 to S2
Caption for Movie S1
References (27-43)
Movie S1

Epigenetic regulators, including ATP-dependent chromatin remodeling enzymes (8-9), are ideally suited to orchestrate the effects of neuronal activity on transcription globally. The ATP-dependent nucleosome remodeling and deacetylase (NuRD) complex triggers alterations of histone modifications, resulting in promoter or enhancer decommissioning and prolonged silencing of transcription (10-15).

To probe the role of the NuRD complex in dynamic regulation of transcription in the brain, we characterized the genome-wide occupancy of the core NuRD ATPase-encoding subunit, Chd4, in the mouse cerebellum. A substantial number of regions (9842) occupied by Chd4 in the cerebellum overlapped with transcriptional start sites (TSS) (fig. S1A). Nearly all Chd4-bound TSS (96%) harbored the histone modification H3K4 trimethylation (H3K4me3), which marks active and poised promoters (16-17), but not H3K27 trimethylation (H3K27me3), which marks inactive promoters (18) (Fig. 1A and fig. S1, B and C). Chd4 binding at H3K4me3-enriched TSS was diminished in the cerebellum in mice in which Chd4 was conditionally deleted in granule neurons (Fig. 1, A and B, and fig. S1, D to H). Chd4 binding at H3K4me3-enriched TSS in the cerebellum correlated tightly with acetylation of H3K9 and H3K14 (H3K9/14ac), which marks actively transcribed loci (19), and with gene expression (Fig. 1C and fig. S1I). Thus Chd4 occupies the promoters of most actively transcribed genes in the mouse brain.

The NuRD complex triggers the sustained repression of only a small set of <200 genes in the cerebellum through diminution of H3K9/14ac and H3K4me3 at these promoters (13). We, therefore, reasoned that the NuRD complex might operate through another epigenetic mechanism to regulate the much larger set of Chd4-bound active genes. Exchange of the histone variant H2A.z is associated with regulation of transcription (20-23). H2A.z was enriched at 97% of Chd4-bound promoters in the mouse cerebellum (fig. S1J). Chd4 knockout decreased H2A.z and acetylated H2A.z enrichment at promoters with high Chd4 occupancy (Fig. 1, D and E), but not at most enhancers in the cerebellum (fig. S2).

We next intersected RNA-Seq (13) and H2A.z ChIP-Seq analyses in the mouse cerebellum of conditional Chd4 knockout and control littermate mice. Although a small group of 121 upregulated genes in conditional Chd4 knockout mice harbored increased H2A.z enrichment at their promoters, a much larger group of 1233 upregulated genes displayed reduced H2A.z enrichment at TSS (Fig. 1F and fig. S3, A and B). Gene ontology analyses revealed that genes with reduced H2A.z enrichment encoded proteins that function in intracellular signaling cascades, cell cycle control, and phosphorylation (fig. S3C). Notably, there was little or no change in H3K9/14ac, H3K4me3, and H3K27me3 or the density of histone H3 at the promoters of these genes upon Chd4 knockout (Fig. 1G and fig. S3, D to G). Together, these data indicate that the NuRD complex triggers the deposition of H2A.z at the promoters of a large group of actively transcribed signaling genes and inactivates their expression in the brain *in vivo.*

The identification of an epigenetic link from the NuRD complex to H2A.z at the promoters of signaling genes led us to determine whether the NuRD complex regulates transcription dynamically in response to neuronal activity. Expression of the activity-dependent genes *c-fos, nr4a1, dusp1,* and *nfil3* was increased in granule neurons of the rodent cerebellum upon

membrane depolarization and rapidly inactivated 1 hour after cessation of membrane depolarization (Fig. 2A). Depletion of Chd4 or Mbd3, another subunit of the NuRD complex (24), impaired inactivation, but not reactivation, of activity genes in neurons after membrane depolarization (Fig. 2A; fig. S4; and fig. S5, A and B). Thus, the NuRD complex appears to be required for inactivation of activity-dependent genes in neurons.

In chromatin immunoprecipitation followed by quantitative PCR (ChIP-qPCR) analyses, H2A.z increased at the promoters of the *c-fos, nr4a1,* and *dusp1* genes in granule neurons during the inactivation phase after membrane depolarization (fig. S5C). Depletion of Chd4 reduced H2A.z enrichment, but not histone H3, at the promoters of the *c-fos, nr4a1,* and *dusp1* genes in neurons during the inactivation phase (Fig. 2B) but not the activation phase (fig. S5D). Thus, the NuRD complex appears to specifically stimulate the loading of H2A.z at the promoters of activity-dependent genes during the inactivation phase of transcription.

Depletion of H2A.z by RNAi in neurons increased expression of the *c-fos, nr4a1, dusp1,* and *nfil3* genes during the inactivation phase of activity-dependent transcription, with little or no effect during activation or reactivation (Fig. 2C and fig. S6). Thus, the NuRD complex and H2A.z are required for inactivation of activity gene expression in neurons.

We next used a rotarod procedure to induce neuronal activity in the mouse cerebellum (Fig. 2D). RNA-Seq analyses from the cerebellum of mice running on a rotarod for 1 hour compared to mice housed in a cage revealed increased transcription of activity genes (Fig. 2E), and these genes were inactivated within 1 hour after rotarod activity stopped. Chd4 knockout increased the expression of *c-fos, fosl2,* and *dusp1* in the cerebellum after cessation of rotarod activity but not during the activation phase of rotarod-induced transcription (Fig. 2F). Thus, the NuRD complex affects specifically the inactivation of activity genes in the brain.

We next tested whether NuRD-dependent inactivation of activity genes might regulate granule neuron connectivity in the cerebellum. We determined the stage of granule neuron maturation *in vivo* during which the NuRD complex regulates activity-dependent transcription. We used *in vivo* electroporation and translating ribosomal affinity purification (25) to characterize gene expression in developmentally synchronized granule neurons *in vivo* (Sync-TRAP) (Fig. 3A and figs. S7, A and B). Sync-TRAP followed by qPCR or by RNA-Seq analyses of the cerebellum in mice 6 days after electroporation revealed that expression of granule neuron-specific genes was enriched (fig. S7C), and led to the identification of chromatin regulators and ubiquitin ligases enriched in developing granule neurons (Fig. 3B and fig. S7D). Sync-TRAP-Seq analyses in $Chd4^{loxP/loxP}$ mice electroporated with the recombinase Cre revealed that 86% of significantly differentially expressed genes were upregulated upon conditional Chd4 knockout (Fig. 3C and fig. S7E). Sync-TRAP-Seq and Sync-TRAP-qPCR analyses revealed transcription of the activity-dependent *npas4, nfil3, c-fos,* and *nr4a1* genes, but not of granule neuron-specific genes, was increased in granule neurons depleted ofChd4 *in vivo* (Fig. 3, D and E). Immunohistochemical analyses confirmed that c-Fos protein was upregulated in Chd4-depleted granule neurons *in vivo* (fig. S8, A and B). Sync-TRAP-qPCR analyses also revealed that depletion of H2A.z increased *c-fos* gene expression in granule neurons *in vivo*

(fig. S8C). The NuRD complex and H2A.z thus appear to trigger the inactivation of activity-dependent genes in synchronously developing granule neurons in the mouse cerebellum.

Because the NuRD/H2A.z epigenetic link regulates activity-dependent transcription in a temporal window of dendrite morphogenesis in the cerebellum, we asked whether NuRD-dependent inactivation of genes might influence dendrite patterning and connectivity. Granule neurons labeled by *in vivo* electroporation undergo distinct stages of dendrite morphogenesis in a synchronized manner *in vivo* (Fig. 4A and fig. S9, A to C). Depletion of Chd4 increased the total length of granule neuron dendrites and the number of primary dendrites during the period of pruning, with little or no effect on the development of granule neuron dendrites during earlier stages (Fig. 4B and fig. S9, A to C). Expression of NuRD-regulated activity genes also impaired dendrite pruning *in vivo* (Fig. 4, C and D). In contrast, upon expression of NuRD-repressed target genes not known to be regulated by activity or other cerebellum-enriched transcriptional regulators, only one increased dendrite length but not dendrite number (Fig. 4, C and D, and fig. S9D). These results indicate that NuRD-dependent inactivation of activity genes may drive granule neuron dendrite pruning in the cerebellum.

We next characterized the consequences of NuRD actions on responses of granule neurons in behaving mice. Mature granule neurons receive on average four mossy fiber inputs, which is optimal for sparse, lossless encoding of sensorimotor information (26). We electroporated mouse pups with a plasmid encoding the calcium indicator GCaMP6s together with an mCherry expression plasmid, and subjected mice to a motorized treadmill task (Fig. 5A, movie S1). After habituation, two-photon imaging of lobule VI in the mouse cerebellum revealed a set of GCaMP6s-labeled granule neurons was active during locomotion (Fig. 5, B and C). Conditional Chd4 knockout triggered a robust increase in the fraction of high-fidelity treadmill-responsive granule neurons, and concomitantly reduced the fraction of unresponsive granule neurons (Fig. 5, C and D). Thus, inhibition of the NuRD complex leads to hyperresponsivity of granule neurons to sensorimotor stimuli.

In behavior analyses, depletion of Chd4 in granule neurons impaired procedural learning including in the accelerating rotarod and delay eyeblink conditioning assays, but had little or no effect on motor coordination as assessed in the DigiGait and open field assays (fig. S10).

Our study defines chromatin remodeling events that inactivate activity-dependent transcription and control dendrite architecture and sensorimotor encoding in the brain (see model in Fig. 5E). Our findings suggest that inactivation of activity genes is essential for the maturation of granule neuron dendrite arbors and in the control of neural circuit activity in response to sensorimotor signals. We have uncovered the NuRD complex and H2A.z as epigenetic regulators that mediate the inactivation of activity genes in the brain. Thus, epigenetic mechanisms may have an active role in the inactivation of gene expression in the brain following neuronal activity.

Supplementary Material

Refer to Web version on PubMed Central for supplementary material.

Acknowledgements

We thank members of the Bonni laboratory for helpful discussions and critical reading of the manuscript, and E. Han for advice in imaging analyses. Supported by NIH grant NS041021 (A.B.), the Mathers Foundation (A.B.), and NIH MSTP grant T32 GM07200 (K.K.H.). We thank the Genome Technology Access Center at Washington University, which is supported by NCI P30 CA91842 to the Siteman Cancer Center and by ICTS/CTSA UL1TR000448.

References

1. West AE, Greenberg ME. Cold Spring Harb Perspect Biol. 2011; 3
2. Spiegel I, et al. Cell. 2014; 157:1216. [PubMed: 24855953]
3. Saha RN, et al. Nat Neurosci. 2011; 14:848. [PubMed: 21623364]
4. Greenberg ME, Ziff EB, Greene LA. Science. 1986; 234:80. [PubMed: 3749894]
5. Qiu Z, Ghosh A. Neuron. 2008; 60:449. [PubMed: 18995819]
6. Ebert DH, et al. Nature. 2013; 499:341. [PubMed: 23770587]
7. Madabhushi R, et al. Cell. 2015; 161:1592. [PubMed: 26052046]
8. Ho L, Crabtree GR. Nature. 2010; 463:474. [PubMed: 20110991]
9. Narlikar GJ, Sundaramoorthy R, Owen-Hughes T. Cell. 2013; 154:490. [PubMed: 23911317]
10. Kaji K, et al. Nat Cell Biol. 2006; 8:285. [PubMed: 16462733]
11. Rais Y, et al. Nature. 2013; 502:65. [PubMed: 24048479]
12. Whyte WA, et al. Nature. 2012; 482:221. [PubMed: 22297846]
13. Yamada T, et al. Neuron. 2014; 83:122. [PubMed: 24991957]
14. Yoshida T, et al. Genes Dev. 2008; 22:1174. [PubMed: 18451107]
15. Fujita N, et al. Cell. 2004; 119:75. [PubMed: 15454082]
16. Bernstein BE, et al. Proc Natl Acad Sci U S A. 2002; 99:8695. [PubMed: 12060701]
17. Santos-Rosa H, et al. Nature. 2002; 419:407. [PubMed: 12353038]
18. Barski A, et al. Cell. 2007; 129:823. [PubMed: 17512414]
19. Shahbazian MD, Grunstein M. Annu Rev Biochem. 2007; 76:75. [PubMed: 17362198]
20. Creyghton MP, et al. Cell. 2008; 135:649. [PubMed: 18992931]
21. Maze I, Noh KM, Soshnev AA, Allis CD. Nat Rev Genet. 2014; 15:259. [PubMed: 24614311]
22. Weber CM, Henikoff S. Genes Dev. 2014; 28:672. [PubMed: 24696452]
23. Rhee HS, Bataille AR, Zhang L, Pugh BF. Cell. 2014; 159:1377. [PubMed: 25480300]
24. Denslow SA, Wade PA. Oncogene. 2007; 26:5433. [PubMed: 17694084]
25. Heiman M, Kulicke R, Fenster RJ, Greengard P, Heintz N. Nat Protoc. 2014; 9:1282. [PubMed: 24810037]
26. Billings G, Piasini E, Lorincz A, Nusser Z, Silver RA. Neuron. 2014; 83:960. [PubMed: 25123311]
27. Williams CJ, et al. Immunity. 2004; 20:719. [PubMed: 15189737]
28. Funfschilling U, Reichardt LF. Genesis. 2002; 33:160. [PubMed: 12203913]
29. Gaudilliere B, Shi Y, Bonni A. J Biol Chem. 2002; 277:46442. [PubMed: 12235147]
30. Bilimoria PM, Bonni A. CSHProtoc. 2008; 2008 pdb prot5107.
31. Yamada T, et al. J Neurosci. 2013; 33:4726. [PubMed: 23486945]
32. Zang C, et al. Bioinformatics. 2009; 25:1952. [PubMed: 19505939]
33. Hotelling H. Ann Math Stat. 1931; 2:360.
34. Wu Y, Genton MG, Stefanski LA. Biometrics. 2006; 62:877. [PubMed: 16984331]
35. Dennis G Jr. et al. Genome Biol. 2003; 4:P3. [PubMed: 12734009]
36. Shalizi A, et al. Science. 2006; 311:1012. [PubMed: 16484498]
37. Yang Y, et al. Science. 2009; 326:575. [PubMed: 19900895]
38. Konishi Y, Stegmuller J, Matsuda T, Bonni S, Bonni A. Science. 2004; 303:1026. [PubMed: 14716021]

39. Holtmaat A, et al. Nat Protoc. 2009; 4:1128. [PubMed: 19617885]
40. Heiney SA, Wohl MP, Chettih SN, Ruffolo LI, Medina JF. J Neurosci. 2014; 34:14845. [PubMed: 25378152]
41. Sheffield ME, Dombeck DA. Nature. 2015; 517:200. [PubMed: 25363782]
42. Ozden I, Dombeck DA, Hoogland TM, Tank DW, Wang SS. PLoS One. 2012; 7:e42650. [PubMed: 22880068]
43. Mellen M, Ayata P, Dewell S, Kriaucionis S, Heintz N. Cell. 2012; 151:1417. [PubMed: 23260135]

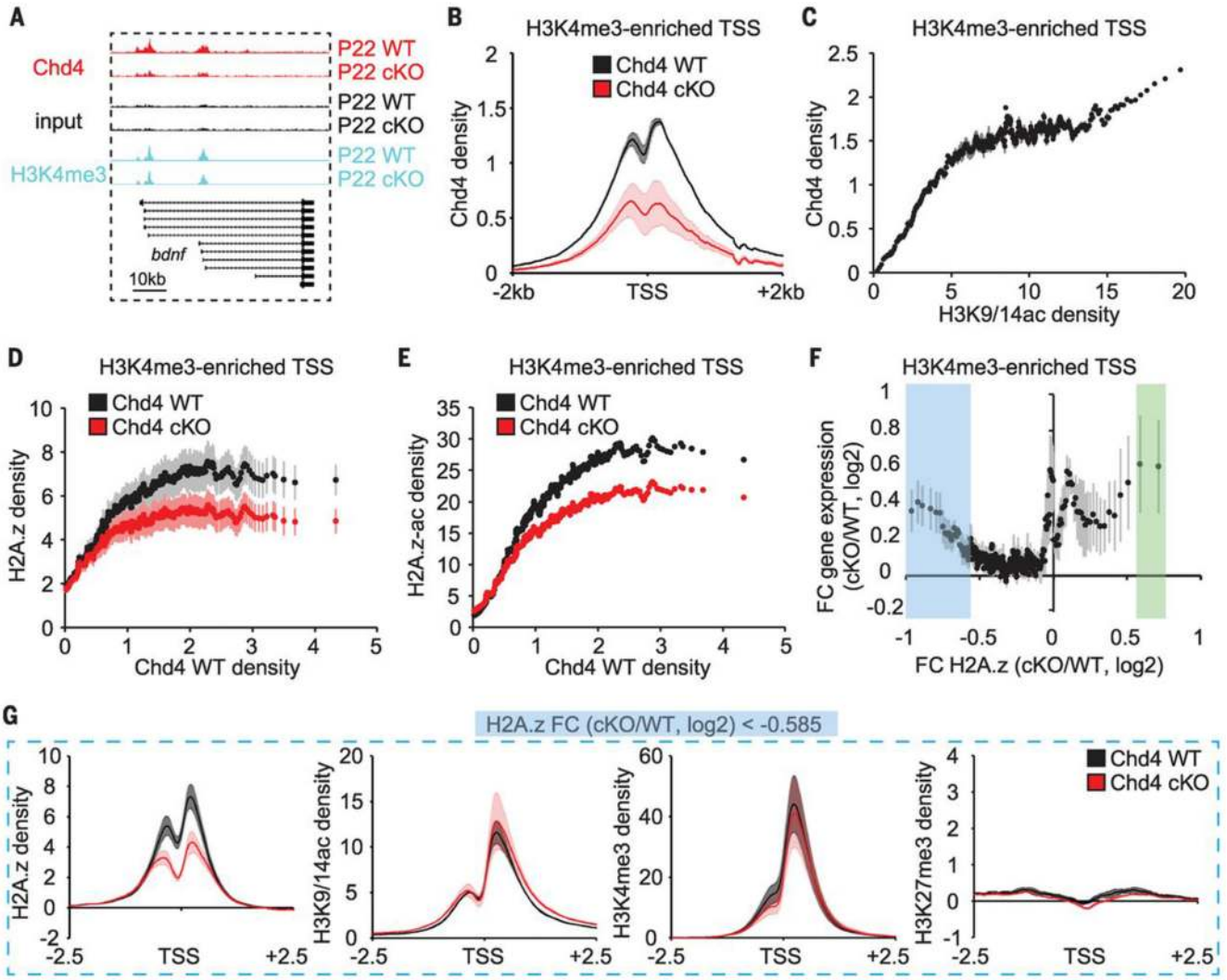

Figure 1. The core NuRD subunit Chd4 occupies promoters of actively transcribed genes in the cerebellum *in vivo*

(A) University of California, Santa Cruz (UCSC) genome browser tracks at the *bdnf* locus in the cerebellum of conditional Chd4 knockout and control mice. **(B)** Location of Chd4 binding near the TSS of H3K4me3-enriched genes in the cerebellum. In all ChIP-Seq analyses, shading denotes standard error. (**C)** Comparison of Chd4 and H3K9/14ac read densities at H3K4me3-enriched genes. **(D** and **E)** Comparison of Chd4 and H2A.z (D, $p<0.01$, Hotelling T^2 test for small sample size) or acetylated H2A.z (E) read density at H3K4me3-enriched TSS in conditional Chd4 knockout and control mice. (**F)** Comparison of the fold change in H2A.z read density and fold change in gene expression at H3K4me3-enriched TSS in P22 conditional Chd4 knockout and control mice. Genes with reduced H2A.z (fold change (log2) < −0.585) upon conditional Chd4 knockout are highlighted in blue, and genes with increased H2A.z (fold change (log2) > 0.585) are highlighted in green. **(G)** The profile of H2A.z, H3K9/14ac, H3K4me3, and H3K27me3 surrounding the TSS of the group of genes indicated in (F) highlighted in blue.

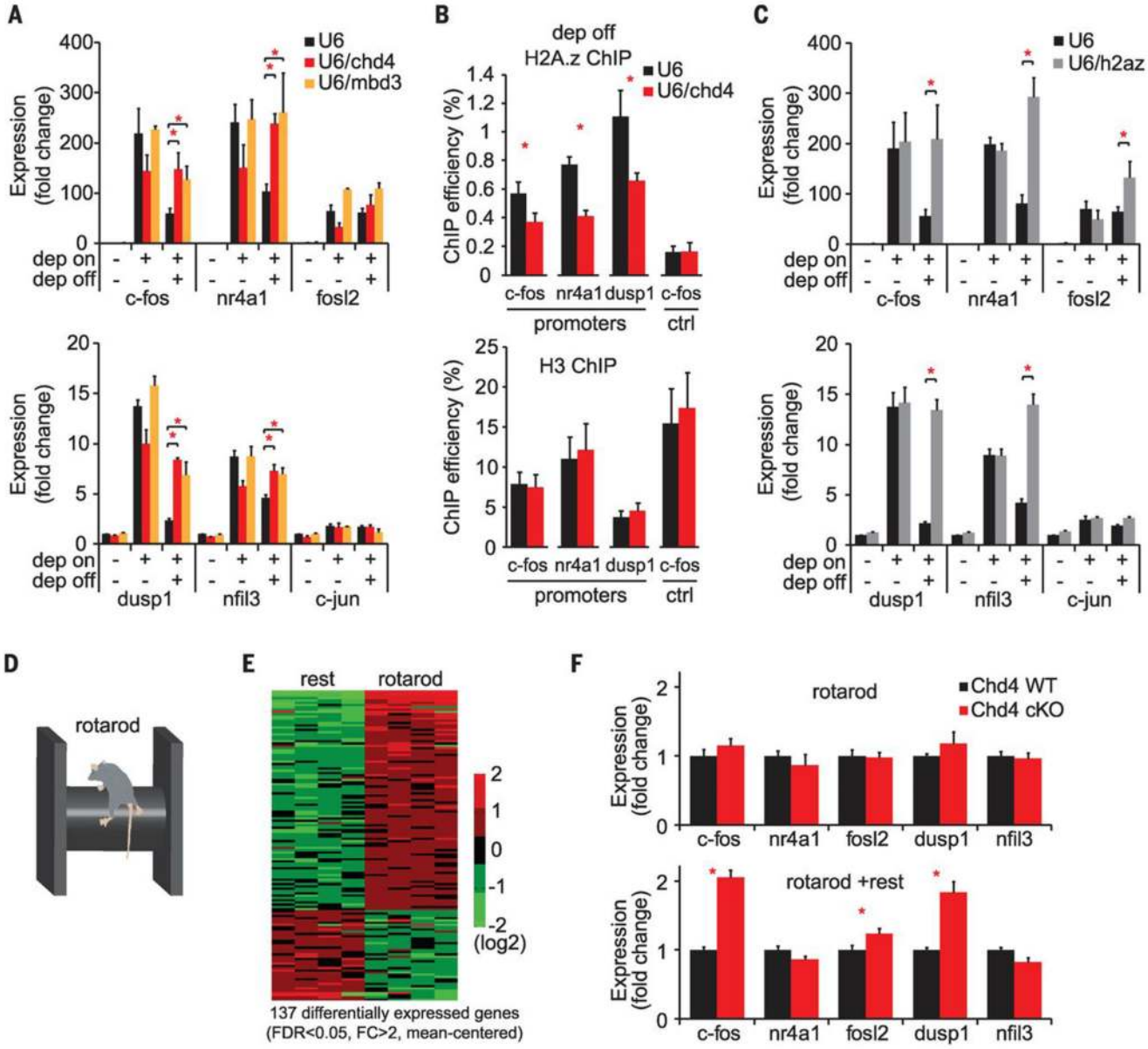

Figure 2. The NuRD/H2A.z chromatin remodeling pathway inactivates activity-dependent genes in neurons

(A) Granule neurons from P5 rat pups transfected with the U6/chd4, U6/mbd3, or the control U6 RNAi plasmid were depolarized (dep on) with 50mM KCl for 1 hour and then switched back to hyperpolarizing media (dep off) for 1 hour and subjected to qRT-PCR analyses. Expression of *c-fos, nr4a1, dusp1,* and *nfil3* genes upon cessation of membrane depolarization in neurons after knockdown of the NuRD subunits Chd4 and Mbd3 (* $p<0.05$, ANOVA followed by Fisher's PLSD post hoc test, n=3). **(B)** Lysates of granule neurons transfected with the U6/chd4 or control U6 RNAi plasmid and treated as in (A) were subjected to ChIP-qPCR analyses using the H2A.z (top) or histone H3 (bottom) antibody and primers specific to the *c-fos, nr4a1,* and *dusp1* gene promoters, or a *c-fos* control region (* $p<0.05$, t-test, n=3). **(C)** Expression of *c-fos, nr4a1, fosl2, dusp1,* and *nfil3*

genes upon cessation of membrane depolarization in granule neurons after knockdown of H2A.z (* p<0.05, t-test, n=3). **(D** and **E)** The cerebellum of P27-P28 mice trained on the rotarod task (D) was subjected to RNA-Seq analyses. A heatmap of the expression levels of significantly differentially expressed genes (E) (FDR<0.05, fold change>2 rotarod compared to control homecage, n=4, base2 log-transformed mean centered). (**F)** The cerebellum of conditional Chd4 knockout or control mice trained on the rotarod task were subjected to qRT-PCR analyses (* p<0.05, t-test, n=6-8 mice).

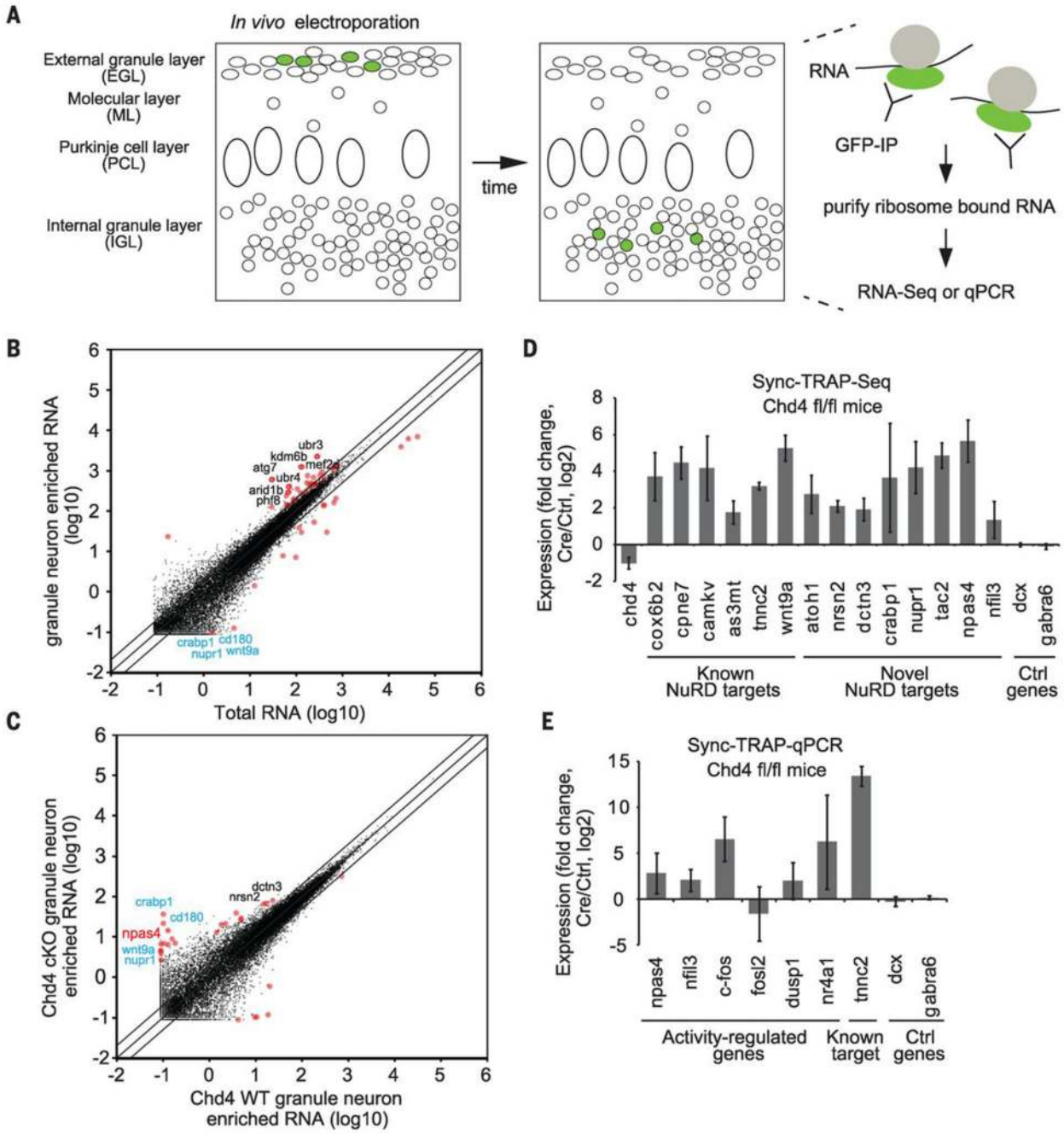

Figure 3. *In vivo* Sync-TRAP analyses reveal that the NuRD complex inactivates activity-dependent genes in synchronously developing granule neurons in the cerebellum

(A) A schematic depicting the Sync-TRAP protocol. *In vivo* electroporation of mouse pups with the GFP-Rpl10a expression vector labels granule neuron precursors localized in the EGL. Labeled granule neurons migrate to the IGL and undergo differentiation in a synchronized manner (see fig. S9A). mRNAs bound to GFP-labeled ribosomes were profiled to characterize the *in vivo* gene expression program in synchronously developing granule neurons. (**B** to **E)** Sync-TRAP followed by RNA-Seq or qPCR analyses using *Chd4*$^{loxP/hxP}$

mice electroporated with the pCAG-Cre or control vector. Scatterplot of input RNA RPKM and immunoprecipitated mRNA RPKM subjected to RNA-Seq analyses (B). Scatterplot of immunoprecipitated mRNA RPKM from Cre-expressing or control granule neurons subjected to RNA-Seq analyses (C). Genes that are less abundant in control electroporated granule neurons compared to input (B) and increased upon knockout of Chd4 compared to control (C) are denoted in light blue. Diagonal lines represent 0.5, 1, and 2-fold changes in the geometric mean of gene expression between conditions (B and C, red circles denote FDR<0.05). Fold changes in gene expression of NuRD targets identified by Sync-TRAP followed by RNA-Seq (D). Validation of NuRD regulated activity-dependent genes using Sync-TRAP followed by qPCR analyses (E).

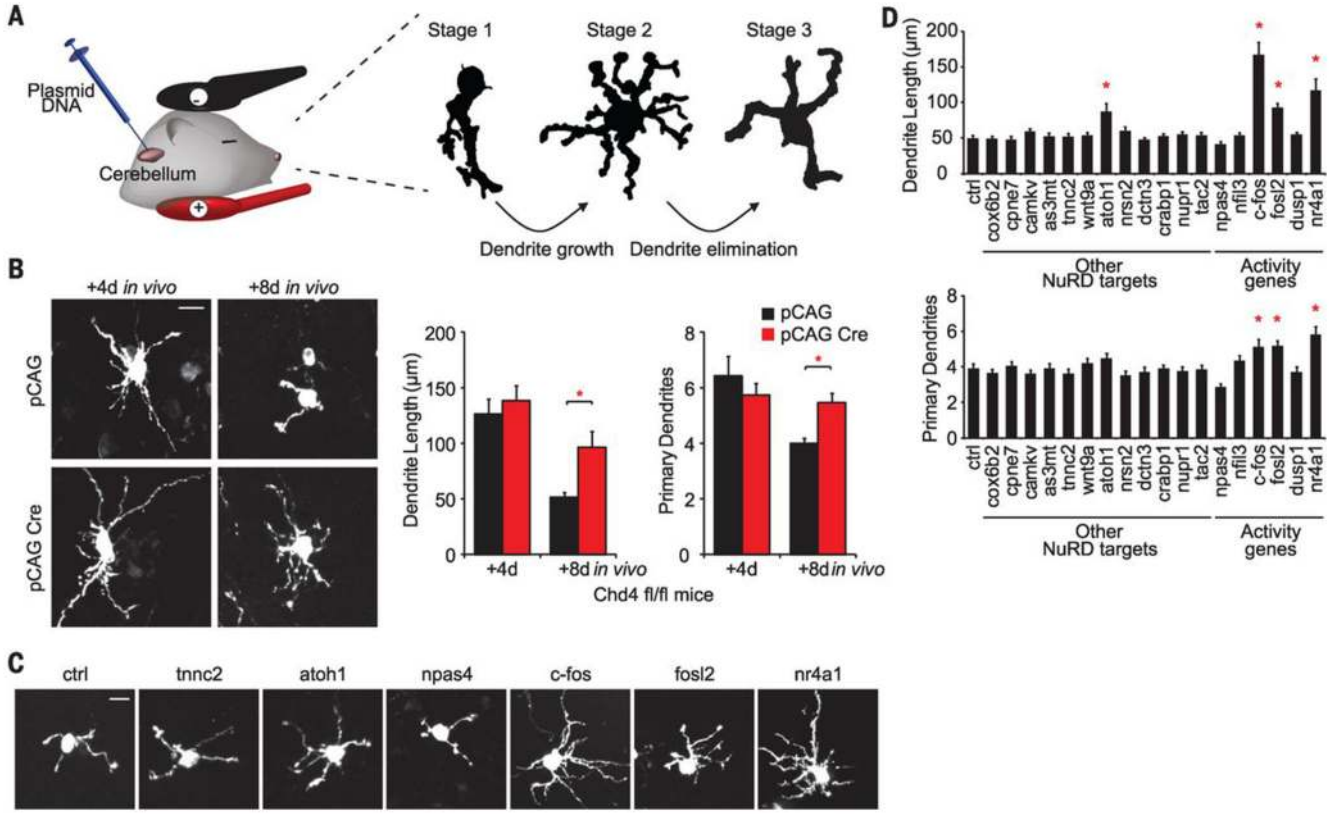

Figure 4. NuRD-dependent inactivation of activity genes drives granule neuron dendrite pruning in the cerebellum *in vivo*

(A) Granule neuron precursors were transfected by *in vivo* electroporation (left), and postmitotic granule neuron morphology was visualized (camera lucida drawings on right). The migration (stage 1), dendrite growth (stage 2), and dendrite pruning (stage 3) of granule neurons are depicted. **(B)** P6 *Chd4*$^{loxP/loxP}$ mice were electroporated with the Cre expression plasmid or control vector together with the GFP expression plasmid and subjected to immunohistochemistry using the GFP antibody. Representative images (left) and quantification (right, * p<0.01, t-test, n=3). **(C** and **D)** P7 rat pups were electroporated with a panel of 6 activity-dependent genes or 12 other NuRD targets and analyzed as in (B). Representative images (C) and quantification (D, * p<0.05, ANOVA followed by Fisher's PLSD post hoc test, n=3-4). Scale bars: 10μm.

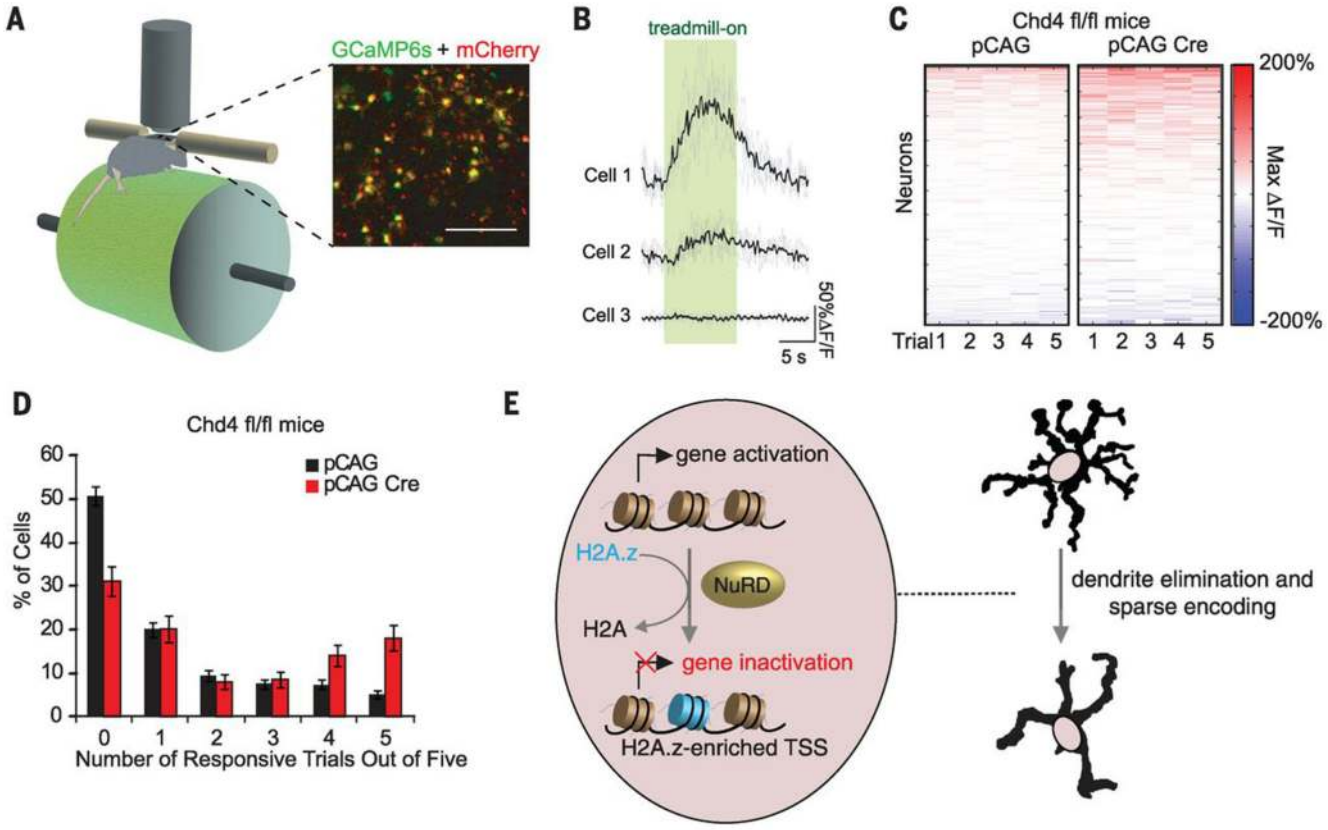

Figure 5. The NuRD complex promotes sparse sensorimotor encoding in behaving mice

(A) Schematic of the paradigm for *in vivo* two-photon calcium imaging during treadmill walking. Granule neurons of lobule VI of the cerebellum electroporated with the GCaMP6s and mCherry expression plasmids (inset). Scale bar: 50 μm. **(B)** Ca^{2+} transients of three representative cells in response to ten second treadmill-on stimulus (Gray: individual trials, black: trial mean, green panel: treadmill-on period). (**C** and **D**) P10-P11 *Chd4*$^{loxP/loxP}$ mice were electroporated with the Cre expression plasmid or control vector together with the GCaMP6s and mCherry expression plasmids. Heat map of maximum ΔF/F (C) and neuronal responsivity distributions (D) during treadmill-on stimulus compared to preceding treadmill-off period for five trials per neuron in conditional Chd4 knockout and control mice (Chi-Square test of independence $p<0.00001$, n=5 mice, 199-520 somas). Error bars represent standard error from bootstrap test. **(E)** Model of the NuRD complex and H2A.z chromatin remodeling link in the regulation of activity-dependent transcription and neural circuit assembly and function.